

1 Magnetism, Magnetic Materials, and Nanoparticles

Adrian Ionescu, Justin Llandro, and Kurt R. A. Ziebeck

1.1 Introduction

Significant changes in the physical properties of materials occur as any of a sample's dimensions are reduced from the bulk ($>50\ \mu\text{m}$) to the nanometer scale. An underlying reason for this change is the increased influence of the surface, for example, the relative contribution of the surface energy to the electrochemical potential.

The electrochemical potential for electrons (also termed the Fermi level) in a solid is a thermodynamic measure (containing the electrostatic contribution) of the energy required to add or remove an electron from the valence band to the vacuum level.

It has been reported that the changes begin when the surface to volume ratio of atoms in the particle approaches 0.5 [1]. If the size of the particle approaches the de Broglie wavelength of the electron (the ratio of the Planck constant, h , to the electron's momentum, p), then quantum size effects can occur. The deviation from bulk behavior and, in particular, the magnetic characteristics, depend not only on the particle size but also on features such as the surface morphology, particle shape, dimensionality, and interactions, among others. For example, the shape of ferro/ferrimagnetic particles influences the preferred direction of their magnetization (magnetic anisotropy) and is therefore crucial for the development of magnetic recording. More recently, magnetic nanoparticles have been used in a range of medical applications, such as drug delivery and MRI contrast imaging, as discussed in Chapter 4, Section 4.2 and Chapter 7, respectively. Their occurrence in natural phenomena, such as sediments and biological organisms, as described in Chapter 8, further enhances their importance. Several comprehensive reviews about synthesis, functionalization, and magnetic properties of nanoparticles are available [1–9]. In most cases, the nanoparticles contain transition metals, and the following discussion will be restricted to this group of materials, although nanoparticles containing rare-earth elements also exhibit a rich variety of magnetic phenomena [10, 11].

1.2 Fundamental Concepts

1.2.1 Quantum Mechanical Concepts

The origins of magnetism arise from quantum mechanical effects. Therefore, a brief introduction to concepts and notation of quantum mechanics is required. Based on the realization in the early twentieth century that particles can behave like waves and vice versa, the theory of wave mechanics was proposed. Combined with the concept of quantization, from the observation that the emission spectra of atoms were composed of spectral lines of discrete energies, a quantum mechanical description of the atom was formulated.

To quantify the discrete energy levels of electrons orbiting around a positively charged nucleus, Erwin Schrödinger proposed a description of the electrons in the atomic orbitals as standing waves, represented by a state or wavefunction ψ . The time-independent Schrödinger equation states that

$$\hat{H}\psi = E_n\psi, \quad (1.1)$$

where \hat{H} is the Hamiltonian of the system including the kinetic and potential energy contributions and E_n is the energy of the n th electron shell. In this description, the Hamiltonian is conceived as an operator, which acts on the wavefunction ψ ; for the Schrödinger Hamiltonian, stationary states (such as electrons in stable atomic orbitals) are the “eigenstates” of the system. This means that if a wavefunction ψ is an eigenstate, the result of the operation of \hat{H} on ψ is simply the same wavefunction ψ multiplied by a proportionality constant, which is E_n . The concept can be extended to time-dependent problems or to slight modifications of the potential energy contribution, which are seen as small perturbations to the stationary case above.

For describing quantum states, one can use the *bra* ($\langle\psi|$)–*ket* ($|\psi\rangle$) notation as introduced by Paul Dirac. For example, the bra, $\langle\psi| = \int_V \psi^*(\mathbf{r}, t) d\mathbf{r}$, could represent the integral over the volume V of the complex-conjugated wavefunction $\psi^*(\mathbf{r}, t)$, which is dependent on the position \mathbf{r} in three-dimensional (3D) space and time t . Conversely, the ket $|\phi\rangle = \int_V \phi(\mathbf{r}, t) d\mathbf{r}$, will be the volume integral over the wavefunction $\phi(\mathbf{r}, t)$. The overlap expression $\langle\psi|\phi\rangle$ will give the probability amplitude of the state ϕ to collapse into ψ .

Measurable quantities or observables in a quantum mechanical system are represented by operators such as \hat{H} , and the probabilistic result of a measurement of the observable is known as the expectation value of the corresponding operator. The expectation value of \hat{H} , when the system is in the state ψ , is defined as $\langle\psi|\hat{H}|\psi\rangle$.

Strictly speaking, solving the time-independent Schrödinger equation yields accurate and discrete energy levels solely for a two-body system, such as an electron orbiting a proton (the hydrogen model). For three or more body problems,

approximations have to be introduced into the potential energy term, reflecting the interaction on each particle by the mean field created by all the other particles (the crystal field). A very widely used approximation is the Hartree–Fock method, which provides the wavefunction and energies for many body quantum systems.

1.2.2 Atomic Magnetic Moments

The magnetic properties of materials can be classified in accordance with their response to an applied magnetic field. This response will usually change as a function of additional external influences, such as pressure or temperature, and except for very low temperatures (< 4 K) it arises from the electronic degrees of freedom (the distribution of electrons into the available energy levels of the atom or the band structure of the solid). In the simplest case, this response may originate from a single isolated atom giving rise to paramagnetism. More complex behavior will arise from atoms coupling in a solid, which can exhibit cooperative phenomena, such as ferromagnetism [12]. A classical picture of the origin of the magnetic moment can be obtained from Ampère’s law, which states that an electric charge in circular motion will generate a magnetic field. In the case of each electron orbiting an atom, there are two contributions to the total magnetic moment. One contribution comes from the motion of the electron around the atomic nucleus, the orbital angular momentum, $\hbar l$, and the other from the electron’s intrinsic angular momentum or spin, $\hbar s$. The orbital moment is

$$\boldsymbol{\mu} = \frac{e\hbar}{2m_e} \boldsymbol{l} = \mu_B \boldsymbol{l}, \quad (1.2)$$

where e is the elementary charge, m_e is the mass of the electron, \hbar is the reduced Planck constant, where $h = 2\pi\hbar$, and we introduce the Bohr magneton μ_B , defined as

$$\mu_B = \frac{e\hbar}{2m_e} = 9.27 \times 10^{-24} \text{ J/T}. \quad (1.3)$$

Equivalently, the Bohr magneton has a value of 5.79×10^{-5} eV/T. For comparison, a magnetic moment of $1 \mu_B$ in a field of 5 Tesla has an equivalent temperature $T = E/k_B \sim 3.4$ K (where E is the energy of the system and k_B is the Boltzmann constant) and so the statistical mechanics of magnetic systems is dominated by thermal energies. The spin moment is

$$\boldsymbol{\mu}_s = g_s \mu_B \boldsymbol{s}, \quad (1.4)$$

where g_s is the electron spin g -factor (approximately 2.002319 [13]).

In a similar fashion to the spin-only situation above, we can define the Landé g -factor g_J for the total angular momentum J :

$$\begin{aligned} g_J &= \frac{J(J+1) - S(S+1) + L(L+1)}{2J(J+1)} + g_s \frac{J(J+1) + S(S+1) - L(L+1)}{2J(J+1)} \\ &\approx 1 + \frac{J(J+1) + S(S+1) - L(L+1)}{2J(J+1)}. \end{aligned} \quad (1.5)$$

The first term in Eq. (1.5) represents the orbital contribution and the second term arises from the electron spin. If the total orbital angular momentum $L = 0$, the Landé g -factor is 2, and if the total spin angular momentum $S = 0$, g_J is 1. Hence the total atomic moment is $\boldsymbol{\mu}_{total} = \boldsymbol{\mu}_{orbital} + \boldsymbol{\mu}_{spin} = \mu_B(\ell + 2\mathbf{s})$. For multi-electron atoms, moment formation occurs through filling the energy levels of the atom in a manner consistent with the Pauli exclusion principle.

The Pauli exclusion principle states that the total quantum mechanical wavefunction of two identical fermions (particles with non-integer spin, such as electrons) must be antisymmetric upon exchange of the two fermions. This implies that not all of the four quantum numbers can be the same for two electrons in an atom.

The four quantum numbers are as follows:

1. the principal quantum number n (an integer representing the energy level or electron shell, alternatively labeled with upper case letters K, L, M, N, O, etc.);
2. the orbital (or azimuthal) quantum number ℓ (representing the subshell, with values ranging from 0 to $n - 1$, conventionally labeled with lower case letters s, p, d, f, g, etc.);
3. the magnetic quantum number m_ℓ (representing a specific orbital within the subshell, and thus the projection of the total orbital angular momentum \mathbf{L} along the z -axis, with values ranging from $-\ell$ to $+\ell$); and
4. the spin quantum number s (representing the projection of the total spin angular momentum \mathbf{S} along the z -axis, with values ranging from $-s$ to $+s$). For example, the 3d electrons reside in the “d” ($\ell = 2$) subshell of the third ($n = 3$, or “M”) shell.

For electrons orbiting an atom, the Pauli exclusion principle requires that two electrons occupying the same atomic orbital must have antiparallel spins.

Except for heavy atoms, the total orbital and spin angular momenta are related by Russell–Saunders coupling [12], governed by $\hbar\mathbf{L} = \hbar\Sigma\mathbf{l}$ and $\hbar\mathbf{S} = \hbar\Sigma\mathbf{s}$. The resultant \mathbf{L} and \mathbf{S} then combine to give the total angular momentum $\mathbf{J} = \mathbf{L} + \mathbf{S}$ as in Figure 1.1. The z -components of \mathbf{J} , m_J , may take any value from $|L - S|$ to $|L + S|$, each $(2J + 1)$ -fold degenerate, thus producing a multiplet in which the separation of the levels is determined by the spin-orbit coupling $\lambda\mathbf{L} \cdot \mathbf{S}$, where λ is the spin-orbit coupling constant. The values of S , L , and J for the lowest energy state are given by Hund’s rules, which are applied in the following sequence:

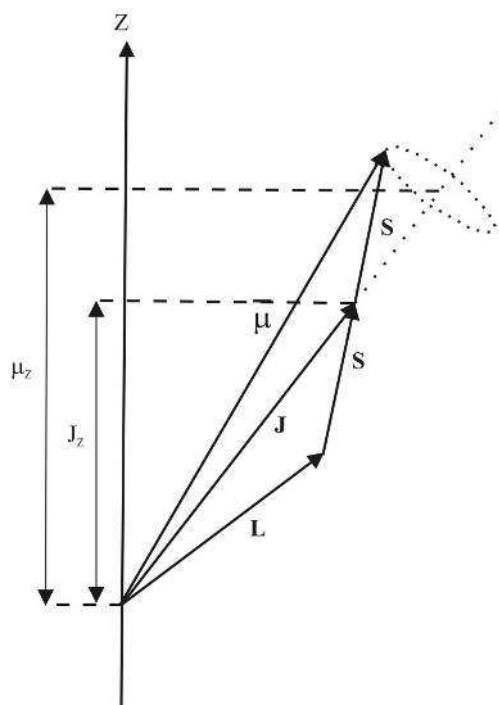


Figure 1.1 The relationship between angular momenta \mathbf{S} , \mathbf{L} and \mathbf{J} and the magnetic moment $\boldsymbol{\mu}$ as well as their projections J_z and μ_z along the z -axis.

1. S takes the maximum value permitted by the Pauli exclusion principle. Each subshell is given one “spin-up” electron before pairing it with a “spin-down” electron, starting from the lowest energy subshell (smallest m_ℓ value).
2. L takes the maximum value consistent with this value of S .
3. For a half filled shell $J = |L - S|$ and for a shell more than half full $J = |L + S|$.

Hund’s rules for electrons in d -orbitals (for which $\ell=2$ and m_ℓ can take the values $-2, -1, 0, 1,$ and 2) in doubly ionized Mn^{2+} , Fe^{2+} , Co^{2+} , Ni^{2+} , and Cu^{2+} (i.e. $3d^5$, $3d^6$, $3d^7$, $3d^8$, and $3d^9$) lead to the following angular momentum and magnetic moments shown in Table 1.1.

It can be seen that the experimental effective Bohr magneton numbers (p_{exp}) are closer to the spin-only values (p_S). However, the situation becomes more complex when the atoms come together to form a solid. Since the $3d$ electrons are the outermost (valence) electrons, they can participate in the bonding. In ionic solids these electrons are perturbed by the inhomogeneous electric field E_c produced by neighboring ions (termed the crystal field or sometimes the ligand field), which breaks the coupling between \mathbf{L} and \mathbf{S} so that the states are no longer specified by \mathbf{J} . Under the influence of the crystal field, the

Table 1.1 Electronic configurations and effective Bohr magneton numbers p_J (total) and p_S (spin-only) for some doubly ionized elements.

	S	L	J	g_J	$p_J = g_J \sqrt{J(J+1)}$	$p_S = g_S \sqrt{S(S+1)}$	p_{exp}
Mn ²⁺	5/2	0	5/2	2	5.92	5.92	5.9
Fe ²⁺	2	2	4	1.50	6.7	4.9	5.4
Co ²⁺	3/2	3	9/2	1.33	6.63	3.87	4.8
Ni ²⁺	1	3	4	1.25	5.59	2.83	3.2
Cu ²⁺	1/2	2	5/2	1.20	3.55	1.73	1.9

$(2L + 1)$ degenerate orbital states in the free atom will be split. If this degeneracy is entirely lifted, then in a non-centrosymmetric field, the orbital angular momenta are no longer constant and may average to zero. This is conventionally called quenching of the orbital angular momentum ($\mathbf{L} = 0$). However, in reality, the differences from the spin-only formula for the magnetic moment still arise from omitting the orbital angular momentum and spin-orbit coupling; hence, we can only really speak of partial quenching ($\mathbf{L} \approx 0$). A more detailed description is given in [14, 15].

If the neighboring ions are treated as point charges, which assumes no overlap or hybridization of their electron orbitals, then the crystal field (or ligand field) potential V_c satisfies Laplace's equation, $\nabla^2 V_c = -\nabla E_c = 0$. Since the electric field $E_c = -\nabla V_c$, this implies that the gradient of the crystal field E_c is constant. Hence, the solutions are the Legendre polynomials, and the potential $V_c(r, \theta, \varphi) = \sum_l \sum_{m_l} A_l^{m_l} r^l Y_l^{m_l}(\theta, \varphi)$ can be

expanded in spherical harmonics $Y_l^{m_l}(\theta, \varphi)$. The energy-level scheme and the occupation are governed by the symmetry of the crystal field, and the relative scales of the energies are given in Table 1.2. Note that the Coulomb interaction between the electrons and the atomic nucleus yields energy level spacings of the order of eVs, much larger than available thermal energies, which allows the total magnetic moment to be thermally stable. For an octahedral field, the five m_l states are split into two groups: a doubly degenerate e_g multiplet and a triply degenerate t_{2g} multiplet, which are separated by the crystal field energy Δ , with the latter multiplet being lower in energy, as shown in Figure 1.2. Their occupation depends on the relative importance of the energy Δ and spin-orbit energy $\lambda(\mathbf{L} \cdot \mathbf{S})$. If $\Delta \gg \lambda(\mathbf{L} \cdot \mathbf{S})$, Hund's rules do not apply, and for Fe²⁺, the six d-electrons pair up and occupy the t_{2g} states producing $\mathbf{S} = 0$. This represents the low-spin or strong-field configuration. For $\Delta \ll \lambda(\mathbf{L} \cdot \mathbf{S})$, the six electrons occupy the t_{2g} and e_g states in accordance with Hund's rules, giving rise to the high-spin or weak-field situation.

If the overlap of the 3d wavefunctions between neighboring atoms is significant, then the electrons that carry the magnetic moments are delocalized (itinerant) and form continuous bands [16]. The magnetic electrons now participate in the conduction and their itinerancy can be characterized by the band width W , that is, the electrons spend a time $t \sim \hbar/W$ in the atom. Thus, the experimental moment values depend on the time constant of the technique used to determine them. The results given in Table 1.3 were obtained from magnetization, neutron diffraction, and X-ray magnetic circular dichroism (XMCD) measurements and represent time-averaged values. It is clear that

Table 1.2 Energy contributions as wavenumbers (spatial frequency of a wave in cycles per unit distance) associated with 3d ions, where $1 \text{ cm}^{-1} = 1.23984 \times 10^{-4} \text{ eV}$. The Coulomb energy provides the ground state, the degeneracy of which can be lifted by the crystal field, the spin-orbit interaction or the Zeeman interaction in the presence of an applied magnetic field $\mathbf{B} = \mu_0 \mathbf{H}$ in vacuum [17].

Coulomb energy	Crystal field	Spin-orbit	Zeeman
	$V_c(r, \theta, \phi)$	$\lambda(\mathbf{L} \cdot \mathbf{S})$	$-g_J \mu_B m_J B$
$10\text{--}40 \times 10^3 \text{ cm}^{-1}$	$10\text{--}20 \times 10^3 \text{ cm}^{-1}$	$100\text{--}800 \text{ cm}^{-1}$	1 cm^{-1}

Table 1.3 Theoretical and observed magnetic moments given in μ_B [18]. The measured X-ray values are compiled from various references given in the reference section.

	$\mu_S(\text{calc})$	$\mu_L(\text{calc})$	$\mu_S(\text{obs})_{\text{neutron}}$	$\mu_L(\text{obs})_{\text{neutron}}$	$\mu_S(\text{obs})_{\text{X-ray}}$	$\mu_L(\text{obs})_{\text{X-ray}}$
Fe	2.21	0.06	2.13	0.08	2.246	0.051
Co	1.57	0.14	1.52	0.14	1.639	0.078
Ni	0.61	0.07	0.57	0.05	0.647	0.051

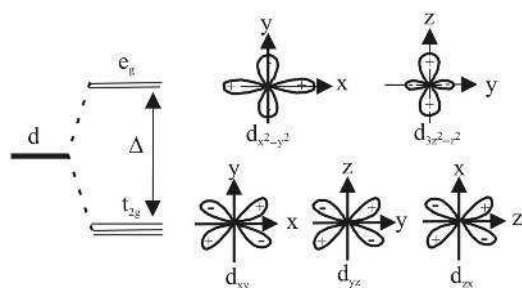


Figure 1.2 The energy levels and associated orbitals of a d electron in an octahedral field split into a doubly degenerate e_g multiplet ($d_{x^2-y^2}$, $d_{z^2-r^2}$) and a triply degenerate t_{2g} multiplet (d_{xy} , d_{yz} , d_{zx}) separated by the crystal field energy Δ .

moments arise predominantly from the spin and are non-integer, a feature explained by band theory. For example, the value for Ni is less than the fundamental unit of $1 \mu_B$. Electronic structure calculations have been carried out using different computational approaches and approximations for the exchange interaction describing coupling between spins (see Section 1.2.4.3 (Exchange Interactions)).

1.2.3 Macroscopic Considerations

In a solid, the periodic arrangement of atoms into a crystal (or lattice) can be described by the repetition of a unit cell containing a certain number of atoms (or chemical formula units) and characterized by a set of lattice parameters a , b , and c (for a cubic unit cell $a = b = c$). It is often more convenient to use the concept of reciprocal (or momentum) space, which correlates the unit real-space lattice vectors \mathbf{x} , \mathbf{y} , \mathbf{z} by Fourier transformation into their reciprocal space counterparts \mathbf{x}' , \mathbf{y}' , \mathbf{z}' [17]:

$$\mathbf{x}' = 2\pi \frac{\mathbf{y} \times \mathbf{z}}{\mathbf{x} \cdot (\mathbf{y} \times \mathbf{z})}, \quad \mathbf{y}' = 2\pi \frac{\mathbf{z} \times \mathbf{x}}{\mathbf{y} \cdot (\mathbf{z} \times \mathbf{x})}, \quad \mathbf{z}' = 2\pi \frac{\mathbf{x} \times \mathbf{y}}{\mathbf{z} \cdot (\mathbf{x} \times \mathbf{y})}. \quad (1.6)$$

The reciprocal space unit cell is called the Brillouin zone; for a simple cubic unit cell with a real-space lattice parameter a , the Brillouin zone is also simple cubic, with a reciprocal lattice parameter $2\pi/a$.

The close proximity of the atoms in the lattice results in significant overlap (hybridization) of atomic orbitals of the outermost electrons, which will form continuous energy bands. The motion of the conduction electrons through the periodic energy landscape can be described using an ideal Fermi gas model, that is, a collection of non-interacting fermions. This motion can be described as a Bloch wave (momentum in a crystal). The Bloch wave has the form

$$\psi(\mathbf{r}) = u(\mathbf{r})e^{i\mathbf{k} \cdot \mathbf{r}}, \quad (1.7)$$

where $u(\mathbf{r})$ is a function with the same periodicity as the crystal and \mathbf{k} is the crystal wavevector related to the crystal momentum $\mathbf{p} = \hbar\mathbf{k}$. The components of $\mathbf{k} = (k_x, k_y, k_z)$ may be related to the real-space lattice vectors by a reciprocal-space transformation as shown in Eq. 1.6. Electrons described by Bloch waves behave almost as free particles in vacuum, just with a modified or effective mass m^* , as long as they reside in parabolic bands, that is, the dispersion relation is $E(\mathbf{k}) = \frac{(\hbar\mathbf{k})^2}{2m^*}$.

For a collection of magnetic moments, for example, in a crystal, the macroscopic magnetization \mathbf{M} is the net magnetic dipole moment per unit volume, defined as $\mathbf{M} = \sum_i \boldsymbol{\mu}_i$,

where $\boldsymbol{\mu}_i$ is the time averaged atomic magnetic moment located on lattice site i . The sum is carried out over all lattice sites in the crystal. The magnetic induction (magnetic flux density) \mathbf{B} is defined in terms of the torque \mathbf{T} exerted on a dipole by a magnetic field: $\mathbf{T} = \boldsymbol{\mu} \times \mathbf{B}$. The units are [N/Am], which can also be written as [Vs/m²], where the volt-second is the Weber (Wb) and so the units become Tesla [T]. The flux density and magnetization are related to the magnetic field \mathbf{H} [A/m] through the equation $\mathbf{B} = \mu_0(\mathbf{H} + \mathbf{M})$, where μ_0 is the vacuum permeability with a value of $\mu_0 = \frac{1}{\epsilon_0 c^2} = 4\pi \times 10^{-7} \left[\frac{\text{Vs}}{\text{Am}} \right]$.

For a macroscopic sample, the magnetization is often linearly proportional to the applied field strength with the constant of proportionality being the magnetic susceptibility χ , $\mathbf{M} = \chi\mathbf{H}$. If the directional dependence becomes important, for example, in a single crystal, the full symmetry of the magnetic susceptibility tensor has to be considered: $\mathbf{M} = \underline{\chi}\mathbf{B}$. Without any additional assumptions, the tensor $\underline{\chi}$ is a 3×3 symmetric matrix with nine independent components. In general, the susceptibility is a tensor quantity and represents the temporal and spatial variation in \mathbf{M} , that is, $\chi = \chi(\mathbf{k}, \omega)$, where the angular frequency ω and magnitude of the wavevector \mathbf{k} are given by the reciprocal relations $\omega = 2\pi/t$ and $k = 2\pi/r$. As will be discussed in Section 1.4.6, the susceptibility can be related to the neutron scattering function, and hence determined by neutron diffraction.

1.2.4 Calculation of Atomic Susceptibilities

The change in the energy of electrons located in an atom in a uniform magnetic field B is given by

$$\Delta E = \mu_B \mathbf{B} \cdot \left\langle \psi_f \left| \hat{\mathbf{L}} + g \hat{\mathbf{S}} \right| \psi_f \right\rangle + \sum_{i \neq f} \frac{\left| \mu_B \mathbf{B} \cdot \left\langle \psi_f \left| \hat{\mathbf{L}} + g \hat{\mathbf{S}} \right| \psi_i \right\rangle \right|^2}{E_f - E_i} + \frac{e^2}{8m} B^2 \left\langle \psi_f \left| \sum_n (\hat{x}_n^2 + \hat{y}_n^2) \right| \psi_f \right\rangle, \quad (1.8)$$

where E_f is the final state (ψ_f) energy, E_i is the initial state (ψ_i) energy, e and m are the charge and mass of the electron, respectively, and \hat{x}_n , \hat{y}_n are position operators defining its spatial coordinates. From this equation, the magnetization and susceptibility can be calculated.

1.2.4.1 Diamagnetism

Based on an atomic application of Lenz's law, which states that a current loop induced by a changing magnetic field produces a magnetic moment, which opposes the applied field, a diamagnetic susceptibility is always negative. All materials show a diamagnetic response but the weakness of the effect means that it is only measurable in the absence of any other magnetic behavior.

For atoms with closed shells, such as He, Ne, and Ar, there is no net spin or orbital angular momentum following Hund's rules. Hence, there is no permanent magnetic moment located on the atom, and for the ground state ψ_0 , the expectation values of the orbital and spin angular momentum operators $\left\langle \psi_0 \left| \hat{\mathbf{L}} \right| \psi_0 \right\rangle = \sqrt{L(L+1)}$ and $\left\langle \psi_0 \left| \hat{\mathbf{S}} \right| \psi_0 \right\rangle = \sqrt{S(S+1)}$ are both zero. The applied magnetic field produces a flux density \mathbf{B} , which in turn causes a screening current to flow and so the magnetization M is obtained from $M(B) = -\frac{1}{V} \frac{\partial E_o(B)}{\partial B}$ and the susceptibility from $\chi = \mu_o \frac{\partial M(B)}{\partial B} = -\frac{\mu_o}{V} \frac{\partial^2 E_o(B)}{\partial B^2}$. The Larmor diamagnetic susceptibility is negative and has the form

$$\chi_{Larmor} = -\mu_o \frac{N}{V} \frac{\partial^2 \Delta E_o(B)}{\partial B^2} = -\mu_o \frac{N}{V} \frac{e^2}{6m} \left\langle \psi_0 \left| \sum_i \hat{r}_i^2 \right| \psi_0 \right\rangle, \quad (1.9)$$

where N is the number of atoms or ions and V the volume. Magnetic susceptibilities are often quoted as molar susceptibilities, based on the magnetization per mole rather than per volume. The conversion is made by multiplying the volume susceptibility by the factor $\frac{N_A}{(N/V)}$, where $N_A = 6.02214086 \times 10^{23}$ is Avogadro's constant. The expectation value $\left\langle \psi_0 \left| \sum_i \hat{r}_i^2 \right| \psi_0 \right\rangle$ is the square of the most probable radius of the outermost electron shell and can only be properly evaluated by a full

quantum-mechanical treatment. However, we can make estimates of the electron shell radius by various means. From semi-classical models of the hydrogen atom, the most probable distance between the proton and the electron can be defined as the Bohr radius $a_0 = 0.529 \text{ \AA}$. For ions of substances like the alkali halides (e.g. F, Br, and Cl) or the solid forms of the noble gases, the mean square ionic radius can be defined as $\langle r^2 \rangle = \frac{1}{Z} \left\langle \psi_0 \left| \sum_i r_i^2 \right| \psi_0 \right\rangle$, where Z is the atomic number (the total number of electrons in the atom or ion), and $\langle (r/a_0)^2 \rangle$ is of order unity. However, for metals, as the electrons are delocalized, a commonly used measure is the free electron radius r_s , which is the radius of a sphere the volume of which is equal to the volume per conduction electron. If the sample of interest has atomic mass A and mass density ρ_m , the number of moles per cubic metre is ρ_m/A (if ρ_m is given in grams per m^3). There are N_A atoms per mole and if each atom contributes Z_i conduction electrons, there are $(N_A Z_i \rho_m)/A$ conduction electrons per unit volume (in m^3). As each conduction electron occupies a sphere of volume $(4\pi r_s^3)/3$, r_s is therefore given by

$$\frac{4\pi r_s^3}{3} = \frac{A}{N_A Z_i \rho_m} \Rightarrow r_s = \left(\frac{3A}{4\pi N_A Z_i \rho_m} \right)^{\frac{1}{3}}. \quad (1.10)$$

Examples of diamagnets are (solid) noble gases, simple ionic crystals, such as alkali halides, graphite, many good metallic conductors (superconductors are perfect diamagnets as they offer no resistance to the formation of current loops), and a number of substrate materials, for example, GaAs. To a first approximation, the contributions of the various ions add for the halides.

Note that, in general, the magnetic susceptibility of conduction electrons is composed of several contributions that are difficult to separate experimentally. For metallic solids, there are two different ‘sources of diamagnetism’, namely the filled electronic shells of the ions (these give rise to the Larmor diamagnetism, as discussed above) and the diamagnetic contribution of the free conduction electrons (which give rise to Landau diamagnetism). The angular momentum in a plane perpendicular to the applied magnetic field is quantized, giving rise to a set of discrete energy levels. The statistical thermal occupation of these Landau levels gives rise to the Landau susceptibility:

$$\chi_{\text{Landau}} = -\frac{2}{3} \rho(E_F) \mu_B^2 \left(\frac{m}{m^*} \right)^2, \quad (1.11)$$

where $\rho(E_F)$ is the density of states (DOS) at the Fermi energy E_F and the last term accounts for the fact that the Bohr magneton is defined for free electrons, rather than those in a band. The Fermi energy is the energy difference between the highest and lowest occupied single particle states at 0 K, and for a metal, it is the energy difference between the Fermi level and the bottom of the conduction band. Except for very low temperatures and high magnetic fields, at which the de Haas–van Alphen effect (oscillations of the magnetic moment in a metal with magnetic field) may be observed, χ_{Landau} is essentially temperature independent.